

CHAPTER 1

ADHESION AND FRICTION OF POLYMERS

Nikolai K. Myshkin and Alexander V. Kovalev

*Department of Tribology, Metal-Polymer Research Institute
Belarus National Academy of Science
Kirov St. 32A, Gomel, Belarus
E-mail: nkmyshkin@mail.ru*

Surface phenomena and the structure of polymers affect essentially their tribological characteristics, the adhesion of polymers to solids being one of the dominating factors. The latter is explained, in particular, by the adsorption (chemisorption) of the functional groups, variations in the polymer crystallinity and morphology, constrained molecular mobility, and catalytic effects of the additives on the reactions occurring in the contact zone. It is shown how load, sliding velocity, and temperature affect friction. Different modes of wear of polymers and friction transfer are considered.

1. Introduction

Friction is a common phenomenon in life and industry, which is governed by the processes prevailing on the surface layers of sliding bodies. The simple idea used in studies of friction is that there are two main components of friction, namely, adhesion and deformation. Such approach is correct for all materials including polymers. The behavior of polymers has distinguishing features, some of which are described by Briscoe.^{1,2} The main concept of the tribology of polymers consists of three basic elements involved in friction:³⁻⁵

- (i) adhesive junctions, their type and strength;
- (ii) shear and rupture of the rubbing materials in the contact;
- (iii) real contact area.

The deformation component of friction results from the resistance of the polymer to “ploughing” by the asperities of the harder counterface. Polymer surface asperities experience elastic, plastic, and visco-elastic deformation depending on the material properties. The adhesion component stems from the adhesive junctions formed on the spots of real contact between the mated surfaces. The adhesion component of friction for polymers is believed to exceed much the deformation. Special consideration is needed for transfer films, being the key factor, which determine the tribological behavior of polymers and polymer composites.

2. Polymers and Polymer Composites

It is known that the size of linear macromolecules of polymers is very big and the main feature of the polymer structure is that macromolecules consist of the rigid segments which can rotate thus providing the flexibility of the molecular chains. Another feature of polymers is that strong chemical forces link the atoms in a polymer chain whereas the intermolecular forces which are significantly weaker, link the chains. The structural features of polymers and the possibility of changing their properties within a wide range provide a variety of the tribological applications of polymers and polymer composites.

The application of the different fillers gives an opportunity of improving the tribological behavior of polymers.⁶ For example; the reinforcement with short fibres (glass or carbon) is used most often to increase the mechanical strength, hence, the load-bearing capacity of polymer composites. Solid lubricants such as polytetrafluoroethylene (PTFE), graphite, molybdenum disulphide added to polymers affect significantly the formation of the transfer films on the counterface and decrease the friction coefficient.⁷⁻⁹

In recent years, owing to rapid advances in nanotechnologies¹⁰, polymer nanocomposites being a polymer matrix filled with the particles 100 nm and smaller in size, have become more and more common. Commonly used nanofillers in plastics are the carbon materials (fullerene and its derivatives), layered clayey minerals, and nanoparticles of metals or their organic and inorganic compounds. Information is available on

the polymer/polymer nanoblends in which the dispersed phase is broken up into the nanometer fragments within the polymer matrix.¹¹

3. Mechanical Behavior of Polymer-Based Materials

The mechanical behavior of polymers is governed by the combination of elasticity and viscosity. At small deformation, polymers behave as the Hook elastic body ($\sigma = E\varepsilon$, where σ and ε are the stress and strain, and E is the modulus of elasticity) modeled with a spring and Newtonian fluid ($\sigma = \eta d\varepsilon/dt$, where η is the viscosity and t is the time); the latter is presented by a damper. The combination of these elements gives a simple description of visco-elasticity (see Table 1).

In general, the constitutive law for polymers is written as the ordinary differential equation with the constant coefficients:

$$a_0\sigma + a_1 \frac{d\sigma}{dt} + \dots + a_m \frac{d^m\sigma}{dt^m} = b_0\varepsilon + b_1 \frac{d\varepsilon}{dt} + \dots + b_n \frac{d^n\varepsilon}{dt^n}, \quad (1)$$

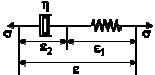


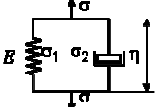
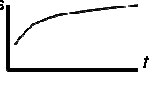
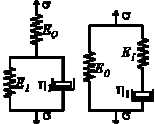
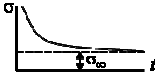
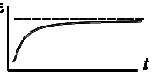
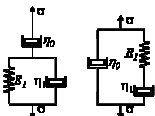
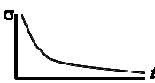
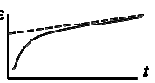
where $a_0, \dots, a_m, b_0, \dots, b_n$ are the constant coefficients governing the mechanical behavior.

4. Adhesion of Polymers

The adhesive bond is formed in two stages. The first stage includes the movement of the polymer molecules towards the solid surface and their certain orientation on it. This process is promoted by the increase in the temperature and the pressure as well as the transition of one of the phases into the liquid state due to its dissolution or melting. If the polymer surface and the counterface are thoroughly cleaned the contact becomes stronger.

The second stage of adhesion involves the direct interaction of the polymer and the solid surface which can be caused by different forces. The covalent forces become predominant at the distances between atoms and molecules not exceeding 0.5 nm; ionic and van der Waals forces are effective at farther distances^{12,13} (approximately from 1 to 100 nm). The interatomic interaction of the contacting phases completes the adhesion process that corresponds to the minimal interphase energy.

Table 1. Simplest models of viscoelasticity.

No	Model	Equation	Relaxation ($\varepsilon=\varepsilon_0$)	Creep ($\sigma=\sigma_0$)
1	<p>Maxwell</p> 	$\frac{d\sigma}{dt} + \frac{1}{\tau}\sigma = E \frac{d\varepsilon}{dt}$		$\varepsilon = \frac{\sigma_0}{\eta} t + \varepsilon_0$ 
2	<p>Kelvin</p> 	$\frac{d\varepsilon}{dt} + \frac{1}{\tau}\varepsilon = \frac{1}{\eta}\sigma$		$\varepsilon = \frac{\sigma_0}{E} \left(1 - \exp\left(-\frac{E}{\eta} t\right) \right)$ 
3	<p>3-element</p> 	$\frac{d\sigma}{dt} + \frac{E_1}{\eta_1}\sigma = (E_0 + E_1) \frac{d\varepsilon}{dt} + \frac{E_0 E_1}{\eta_1} \varepsilon$		$\varepsilon = \varepsilon_\infty - \frac{\sigma_0}{E_1} \exp\left(-\frac{E_1}{\eta_1} t\right)$ 
4	<p>3-element</p> 	$\frac{d\sigma}{dt} + \frac{E_1}{\eta_1}\sigma = \eta_0 \frac{d^2\varepsilon}{dt^2} + E_1 \left(1 + \frac{\eta_0}{\eta_1} \right) \frac{d\varepsilon}{dt}$		$\varepsilon = \frac{\sigma_0}{\eta_0} t + \frac{\sigma_0}{E_1} \left(1 - \exp\left(-\frac{E_1}{\eta_1} t\right) \right)$ 

The bonds formed between the contact surfaces are followed by junctions appearing on real contact spots. The formation and rupture of the junctions govern the adhesion component of friction. The simple model of junction formation has been proposed by Bowden and Tabor.³ For the majority of polymers van der Waals and hydrogen bonds are typical.^{14,15} The hydrogen bond exists at a very short distance in the polymers containing the chemical groups where the hydrogen atom is linked with an electronegative atom.

The junctions sheared under the applied tangential force result in the friction force. In general, the interfacial junctions are influenced by the nature of the mated surfaces as well as by the surface chemistry and the stresses in the surface layers.

If the interfacial bonding is stronger than the cohesive strength of the weaker material, the latter is fractured and the polymer transfer takes place. Otherwise, fracture occurs at the interface. According to well accepted phenomenon, in polymers the surface forces and the forces acting between the polymer chains are nearly equal and fracture often occurs in the bulk of polymers. But, it was observed for metal-polymer contact that the metal is transferred to the polymer surface under certain conditions.^{14,15}

Tsukruk¹⁶⁻¹⁸ *et al.* described the formation of stable molecular lubrication films from the functionalized tri-block copolymer with poly[styrene-*b*-(ethylene-co-butylene)-*b*-styrene (SEBS). This polymer was chemically deposited to the silicon oxide surface covered with the interfacial epoxy-terminated monolayer. The authors optimized the grafting density and thickness of the SEBS films to assure the development of organized structure within the molecularly thick (~10 nm) films. The key components of this microstructure, which, the authors believe, are critical for obtaining the superior interfacial properties, are the 2D net of interconnected glassy polystyrene nano-domains reinforcing the resin matrix and the dense chemical grafting of the resin matrix to the substrate. These SEBS films with optimal microstructure show tribological properties far exceeding those of other molecular coatings and self-assembled monolayers. They possess a very low friction coefficient, modest adhesion, and the superior wear stability compared with the non-structured or non-reinforced organic lubricating coatings.

4.1. Thermodynamic Approach (Specific Surface Energy)

When two solids approach one another it is just the interactions of their molecular fields that result in the attraction forces. Strong adhesion requires deformation at contact points to be plastic since in elastic contact the stored potential energy can rupture the junction when the

contact is unloaded. The thermodynamic work of adhesion between solids 1 and 2 equal to the work of reversible adhesion rupture is determined by the Dupre formula:

$$\gamma = \gamma_1 + \gamma_2 - \gamma_{12} , \quad (2)$$

where γ_1 and γ_2 are the energies required to form the unit surfaces of solids 1 and 2 (their free energy) and γ_{12} is the excessive or interphase energy.

When discussing the surface phenomena it is necessary to distinguish the work required to form a unit surface and the work required to expand the available surface S by the same area. This means that the surface energy and surface tension are different characteristics.¹⁹ The surface energy γ_s and surface tension σ_s are related by the known expression:

$$\gamma_s = \sigma_s + S \frac{\partial \sigma_s}{\partial S} . \quad (3)$$

In general, the difference between σ_s and γ_s can be considerable for liquids and negligible for crystalline solids if the experiment is performed at elevated temperatures and lasts for a long time.

4.2. Contact Adhesion

Several models have been developed to describe the contact adhesion. The Johnson-Kendall-Roberts (JKR) model^{20,21} sometimes referred to as the model of contact mechanics and the Derjaguin-Muller-Toporov (DMT) model²² are best known. The comparative analysis of the models²³ shows that the JKR model is applied to the bodies of micrometer and greater sizes having the properties of polymers, whereas the DMT model is valid for bodies of nanometer sizes having the properties of metals. Therefore, we briefly discuss below the JKR model.

The JKR model is based on the assumption on an infinitely small radius of effect of surface forces, i.e. it is assumed that interactions occur only within the contact area. Elastic contact between a sphere of radius R and half-space is analyzed with consideration of van der Waals forces which compress the mated bodies together in addition to the applied load. The energy of molecular interactions is $W_m = -\pi a^2 \gamma$. The contact

stiffness resists the action of the forces. Using energy balance the equations for the main contact parameters are derived based on the combination of the Hertzian pressure distribution (loading) and Boussinesq distribution (unloading). Such combination yields the compression in the middle of the contact and an infinite tensile stress at its edges.

The formula for calculating the radius of adhesive contact is

$$a^3 = \frac{R}{K} \left(P + 3\pi R\gamma + \sqrt{6\pi R P \gamma + (3\pi R\gamma)^2} \right), \quad (4)$$

where $K = \frac{4}{3} \frac{1-\nu^2}{E}$ is the elastic constant, E is Young's modulus, and P is the normal load.

Therefore, it is apparent that without adhesion ($\gamma = 0$) the Hertz equation is obtained while if $\gamma > 0$ the contact area always exceeds that of the Hertzian contact area under the same normal load P . We note that when the contact is fully unloaded ($P = 0$) it does not disappear but remains finite with the radius

$$a = \left(6\pi R^2 \gamma / K \right)^{1/3}. \quad (5)$$

Only the application of a tensile (negative) load can reduce this radius, and then the contacting surfaces would separate at the least load corresponding to the conversion of the radicand in Eq. (4) into zero

$$P_{\text{pull-off}} = -\frac{3}{2} \pi R \gamma. \quad (6)$$

This circumstance is the specific feature of the JKR model.

Derjaguin was the first (1934) to formulate and solve approximately the problem of the effect of elastic contact deformation on adhesion. Later on Derjaguin, Muller, and Toporov developed it further in their works resulting in creating the DMT model describing the contact of an elastic sphere with a rigid half-space. This model is based on the following two postulates: surface forces do not change the deformed profile of the sphere and it remains Hertzian; the attraction force acts outside the contact circle pressing the bodies together with the contact

region being under compression by the stresses distributed according to Hertz.

Equilibrium is reached when the deformation is sufficient for the elastic response (the force of elastic restoration of the sphere) F_e to counterbalance the joint effect of the applied external load P and the forces of molecular attraction F_s :

$$F_e = P + F_s . \quad (7)$$

Let us assume that attraction is represented by the Lennard–Jones potential. The profile of the deformed sphere outside the contact area for a given radius r is known to be described by the equation

$$z(r, a) = \frac{1}{\pi R} \left[a(r^2 - a^2)^{1/2} - (2a^2 - r^2) \arctan \left(\frac{r^2}{a^2} - 1 \right)^{1/2} \right] \quad (8)$$

to which the equilibrium state z_0 (the clearance within the contact site) should be added. Then the molecular attraction force is calculated by the direct integration:

$$F_s = 2\pi \int_a^\infty p(z + z_0) r dr .$$

The calculation of this integral is rather difficult yet the number of approximate formulas have been published which facilitate the use of the model in question. In particular, there is a simple Maugis relation between the load and approach obtained for the conditions of the DMT model²⁴:

$$\frac{P}{P_c} = \frac{1}{\sqrt{3}} \left(\frac{\delta}{\delta_c} \right)^{3/2} - \frac{4}{3} , \quad (9)$$

where δ is elastic displacement, $P_c = \frac{3}{2} \pi \gamma R$, $\delta_c = \left(\frac{P_c^2}{3K^2 R} \right)^{1/3}$.

Analysis shows that each of these models is true for the certain combinations of physical-mechanical and geometric characteristics of the bodies (see Fig. 1). The DMT theory is applicable to the materials for which the point with the coordinates (K, γ) lies below the corresponding

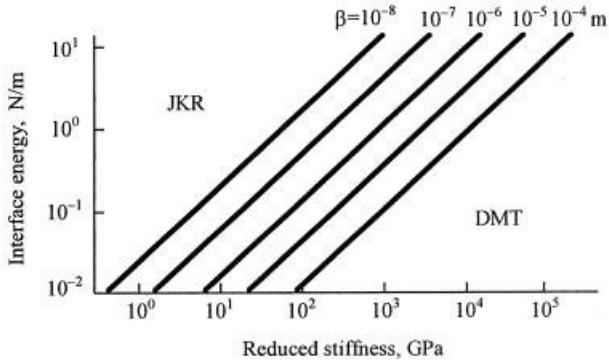


Fig. 1. Domains of parameters (K , γ) where either of two models (JKR or DMT) is correct.

line plotted at the constant radius of asperity tip β . Here K is the reduced stiffness of the contacting materials and γ is the interface energy.

4.3. Contact of Rough Surfaces

When two surfaces approach each other their opposing asperities with the maximum heights come into contact forming the individual spots. The total area of these spots is known as the real contact area (RCA).

When simulating the real contact in the case of plastics, the temperature and sliding velocity should be taken into account^{3,25-27}.

Let us consider the contact of rigid rough body and a smooth elastic half-space.^{27,28} The half-space is taken to be homogeneous and isotropic with the Young's modulus E , Poisson's ratio ν , and the thermal expansion coefficient α . The problem for a heated sphere of the radius R was solved by Barber²⁹ under the following assumptions: the temperature of the heated sphere is T while outside the contact the surface of the half-space is free of the mechanical and thermal loads.

The desired solution, i.e. the relationship between the total load P , circular contact radius a , and approach of the sphere δ is sought as a superposition of the solutions for the problems considering mechanical loading and heating.

Following the Greenwood-Williamson approach³⁰, we can be able to find the total area of all contact spots (RCA) and the total load. The non-dimensional equations for the normal distribution of the asperity heights are written as follows:

$$A_r / A_a = \pi R D \sigma_r \frac{1}{\sqrt{2\pi}} \int_h^\infty (\xi - h) \exp[-\xi^2 / 2] d\xi, \quad (10)$$

$$\begin{aligned} \frac{P}{A_a} \frac{(1-\nu^2)}{E} &= \frac{4}{3} R^{1/2} D \sigma_r^{3/2} \frac{1}{\sqrt{2\pi}} \int_h^\infty (\xi - h)^{3/2} \exp[-\xi^2 / 2] d\xi \\ &+ \frac{2\alpha T}{\pi} (1+\nu) R D \sigma_r \frac{1}{\sqrt{2\pi}} \int_h^\infty (\xi - h) \exp[-\xi^2 / 2] d\xi. \end{aligned} \quad (11)$$

Here A_a is the apparent contact area, A_r is the real contact area, D is the surface density of asperities, σ_r is the root-mean-square roughness, α is the bandwidth parameter, ξ is the non-dimensional height of asperity, and h is the non-dimensional separation.

In a study by Petrokovets (1999)²⁸ it was shown that the RCA of two bodies with different temperatures becomes smaller when the temperature difference increases, and the RCA is always smaller than in the isothermal case. However, if the mechanical behavior of the material is sensitive to temperature changes, the above RCA decrease may be “hidden” by RCA rise due to the reduction in the mechanical characteristics of the material.

If the rheological behavior is governed by a single relaxation time, the simple exponential dependence describes its temperature-dependent modulus:

$$E = E_0 \exp(-\beta T) \quad (12)$$

where β is a constant having dimension of the reciprocal of the temperature and conventionally termed as the rheological parameter.

The calculation was performed under several loads with different values of β . Some results are presented in Fig. 2. It is seen that the temperature-dependent RCA may pass the minimum with increasing the temperature. The existence of this minimum and its value depend on the combination of the thermal (α) and mechanical (rheological)

properties of the contacting materials. Increase in the rheological parameter β , i.e. the sharpening of the temperature dependence of the modulus, results in degeneration of the minimum (the ascending RCA ~ E curve) all other things being the same (see Fig. 2).

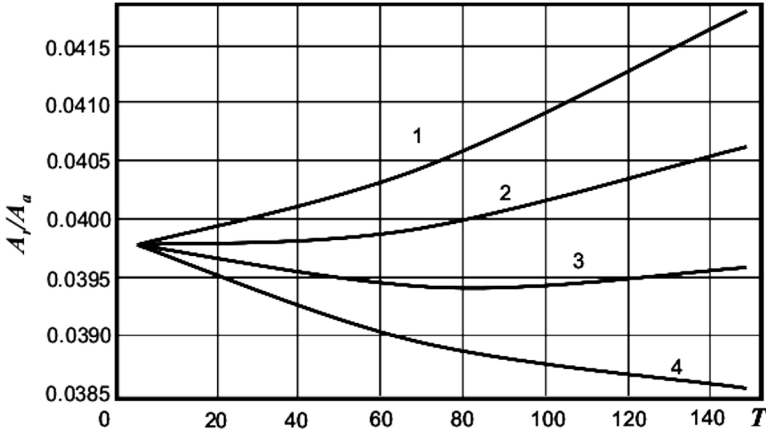


Fig. 2. Effect of the rheological parameter β on temperature-dependent real contact area A_r/A_a : 1 - $\beta = 0.0020$; 2 - 0.0018, 3 - 0.0016; 4 - $\beta = 0.0014$.

4.4. Contact of Rough Surfaces with Adhesion

It is commonly known that the real surfaces are rough. Experiments show that the roughness affects the adhesion of rough surfaces to a large extent. As an example, contact between a sphere and a rough half-space is considered. The analysis is based on the Greenwood and Tripp model³¹ where the load-approach relation is treated as in the case of a single asperity. It can be shown that the total force acting on the sphere is

$$P = 2\pi P_c D \int_0^{a^*} \int_0^\infty r \bar{P}_i(z-h) \Phi_\alpha(z) dz dr.$$

After the change of variables and transformations the force P becomes

$$P = P_c \frac{3\sqrt{2}}{8} \pi \Delta_c \mu \sqrt{\frac{\beta}{R}} I(h, \alpha, \Delta_c), \quad (13)$$

where $P_c = \frac{3}{2} \pi R \gamma$ is the adhesion of the smooth sphere of the radius R ;

$\mu = \frac{8}{3} D \sigma_r \sqrt{2R\beta}$ is the complex parameter of surface topography;

$$I(h, \alpha, \Delta_c) = \int_0^{a^*} \int_0^{\infty} \bar{P}_1(x) \Phi_{\alpha}^*(h + a_0 y + b_0 y^2 + \Delta_c x) dx dy$$

$$h = d / \sigma_r; a_0 = 1 - \zeta / c; b_0 = \frac{3}{2} \left(k - \frac{1}{2}\right) \frac{\zeta}{c^3};$$

$$\zeta = \frac{\sqrt{\pi}}{4} \mu F_{3/2}(h, \alpha) \Gamma(k+1) / \left(k + \frac{1}{2}\right);$$

$$a^* = \frac{3}{4} \sqrt{\pi} c \Gamma\left(k + \frac{3}{2}\right) / \Gamma(k+2); F_{3/2}(h, \alpha) = \int_h^{\infty} \Phi_{\alpha}^*(\xi) d\xi.$$

Here $\Delta_c = \delta_c / \sigma_r$ is the adhesion parameter, and $\Phi_{\alpha}^*(\xi)$ is the Nayak distribution of asperity peaks.³²

Thus, Eq. (13) allows the force compressing two rough surfaces to be estimated. It describes the situation where the contact is unloaded. After unloading the compressive force is zero whereas the separation remains non-zero and has the definite value h_0 which is found from the condition

$$I(h_0, \alpha, \Delta_c) = 0. \quad (14)$$

In order to detach the surfaces fully ($h_0 = 0$), the certain negative (tensile) force should be applied. Then due to adhesion the asperities with the initial height h_0 are lengthened by δ_c which is found from Eq. (14) where the lower limit of the integration is replaced with $-L$ ($L = \min(\Delta_c, h - h_0)$). The minimal value of P is the pull-off force (adhesion force). The calculations have indicated that the roughness initiates sharp decrease in the adhesion. For example, if the root-mean-square roughness σ_r increases twice the adhesion drops by about two orders of magnitude. This effect of the roughness cannot be explained by the reduction of the contact area. It can be attributed by the successive rupture of adhesive junctions at the elastic recovery of the highest asperities during the separation of the contacting surfaces. Some results of the calculations for the contact of polymers are in satisfactory

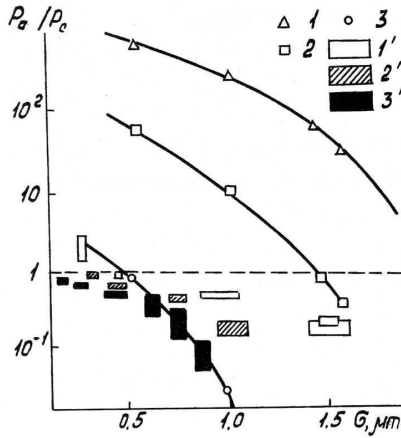


Fig. 3. Effect of roughness on adhesion: 1, 1' - $K = 0.29$ MPa, $\gamma = 0.068$ N/m, $\Delta_c = 1.99$ - 6.49 ; 2, 2' - $K = 0.91$ MPa, $\gamma = 0.040$ N/m, $\Delta_c = 0.66$ - 2.14 ; 3, 3' - $K = 3.20$ MPa, $\gamma = 0.034$ N/m, $\Delta_c = 0.26$ - 0.84 ; 1-3 - calculation, 1'-3' - experiment.

agreement with the data obtained in the experiments of Fuller and Tabor³³ (see Fig. 3).

There is no question that the surface asperities are not smooth, i.e. they have smaller asperities of the nanoscale size which result from the molecular and supramolecular structure of polymers. In this case the RCA should be estimated based on the two-level model of Archard type. To take into account microroughness on large asperities the solution of Greenwood and Tripp³¹ for the contact of two rough spheres is used as the governing equation for a single asperity. Analysis of the two-level model has shown that the highest asperities of the first level (roughness) are coming into contact and form the individual contact spots. Yet, contrary to traditional view, the spots are not continuous but multiple connected, that is, each spot consists of a set of smaller spots whose total area is conditionally named the "physical contact area". This area is less than the real contact area by an order of magnitude. Taking into account the height distribution of asperities, the dependence of dimensionless contact area on dimensionless load is obtained in parametric form:

$$\tilde{A} = 3^{1/3} \Delta_c I(h, \alpha, \Delta_c)$$

$$\tilde{p} = 3^{1/3} \Delta_c^{3/2} I(h, \alpha, \Delta_c).$$

On the other hand, for the two-level model (roughness plus subroughness) the calculation of the contact area revealed that it may increase several times due to the effect of the surface force (see Fig. 4).

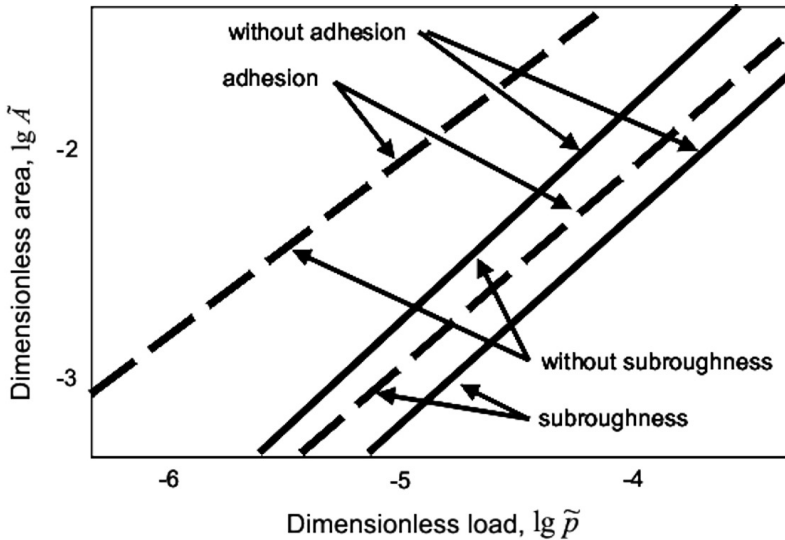


Fig. 4. Effect adhesion on discrete contact area.

The two-level model with adhesion is of interest for precision engineering. It can be developed in the same manner as in the above case. A rough sphere models the asperity of the first level. The load-contact radius relation for a single microasperity is assumed to result from the JKR or DMT theory. The calculation procedure is described elsewhere.^{34,35}

4.5. Measurement of Adhesion

A modern instrument for measuring adhesion is the surface forces apparatus (SFA). The SFA allows one to measure directly the laws of forces in liquids and vapors.^{36,37} It contains two crossed atomically smooth mica cylinders. One mica cylinder is mounted to a piezoelectric translator, through which the distance is adjusted. The other mica cylinder is mounted to a spring with the known and adjustable spring

constant. The separation between the surfaces is measured optically using the multiple beam interference fringes. Knowing the position of one cylinder and the distance to the surface of the second cylinder the deflection of the spring and the force can be calculated.

One of the main problems arising when measuring molecular forces is that they increase rapidly with shortening the distance between the specimens under testing. Hence, the measurements should be carried out at a very low speed that can not be provided by the design of the common balance.

Derjaguin *et al.* proposed to solve the problem¹³ by applying the principle of a feedback balance. Following this idea we have developed a new apparatus for studying surface forces – the contact adhesion meter³⁸ (see Fig. 5).

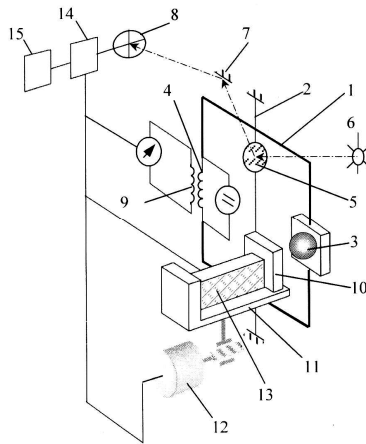


Fig. 5. Principal scheme of adhesion meter: 1 – frame; 2 – string; 3 – holder; 4 – movable coil; 5 – mirror; 6 – laser; 7 – expander of optical base; 8 – photodetector; 9 – coil; 10 – specimen; 11 – table; 12 – stepping motor; 13 – system of fine positioning controlled by piezodrive.

The device consists of a ball probe fixed on the arm of a highly sensitive electromagnetic balance with negative feedback. The dependence of adhesion forces on the distance between the ball probe and the sample is measured in both approach and pull-off modes. The interface forces which tend to rotate the arm with the ball are

compensated by an electromagnet placed on the opposite arm of the balance. The measurement of the compensating current in the electromagnet allows us to determine the acting interface forces.

The contact adhesion meter (CAM) is capable of measuring the force interaction of surfaces in two regimes. When the surfaces are separated the rupture of bonds (pull-off force) is obtained. The whole process is shown in Fig. 6 which presents the force-distance curve.³⁹ In the Fig. 6 the point A shows the beginning of the interaction of the approaching surfaces, the portion AB corresponds to pure attraction without formation of the real mechanical contact between the solids. To the left from the point B the force interaction and elastic deformation occur simultaneously. At the point C the elastic force of resistance to penetration becomes dominating. The point D corresponds to the moment when the elastic force of resistance to penetration equals the adhesive force of the mutual attraction.

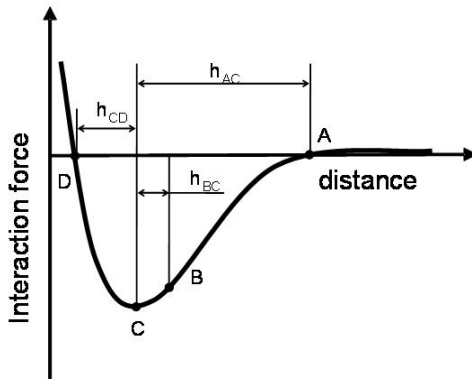


Fig. 6. Stages of contact formation and main points on force-distance curve: h_{AC} – effective radius of surface forces; h_{BC} – corresponds to tensile elastic deformation of surface; h_{CD} – corresponds to elastic mutual penetration with account for adhesive attraction between solids.

We have measured the surface energy of coatings on a silicon plate (crystal structure (111), homopolar semiconductor). The coatings were 3 nm thick octadecyltrichlorosilane (OTS), 8 nm thick poly[styrene-*b*-(ethylene-co-butylene)-*b*-styrene (SEBS), and 1 nm thick epoxysilane.

Also the organic SAMs (self-assembled monolayers) of ODPO₄ (octadecylphosphoric acid ester) and DDPO₄ (dodecylphosphoric acid ester) 2 nm thick with the titanium and titanium oxide underlayers were studied. The silicon and titanium balls with the radius of 1 and 1.5 mm, respectively, were used as probes.

These measurements^{39,40} have demonstrated that the specific surface energy of the studied coatings depends on the coating and probe materials as well as the probe radius. It is 0.004 J/m² for OTS and epoxysilane (probe radius 1 mm) and 0.003 J/m² for epoxysilane and 0.002 J/m² for SEBS (probe radius 1.5 mm). The following results were obtained for SAMs: 0.007 J/m² for Si/TiO_x/ODPO₄, 0.011 for Si/Ti/ODPO₄, and 0.002 for Si/Ti/DDPO₄ (probe radius 1 mm), and 0.004 J/m² for ODPO₄ (probe radius 1.5 mm).

5. Friction of Polymer over the Hard Counterface

Several authors^{4,41-49} have studied the state of art in polymer tribology. The hardness, plasticity index (which describes the deformation properties of rough surfaces), and elastic modulus were obtained for organic polymers (poly(methylmethacrylate), PMMA; poly(styrene), PS; poly(carbonate), PC; ultra-high molecular weight poly(ethylene), UHMWPE) using the contact compliance method.⁵⁰ The dependence of the imposed penetration depth, the maximum load, and the strain rate upon the hardness and elastic modulus was described;^{51,52} typical penetration depths were in the range from about 10 nm to 10 μm while the applied loads were less than 300 mN.

It should be noted that almost without exception ploughing is accompanied by adhesion and under certain conditions it may result in microcutting, that is, an additional work should be done increasing the friction force.

There are other mechanisms of energy dissipation at deformation. For example, when a polymer with visco-elastic behavior slides over a hard rough surface energy dissipation is caused by the high hysteresis losses. This deformation component is known as friction due to the elastic hysteresis.^{3,53} The energy may also be carried away, for example, with elastic waves generated at the interface and outgoing to the infinity,

owing to the nucleation and development of microcracks in the material.^{1,54}



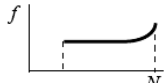
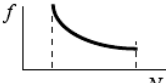
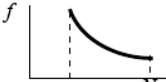
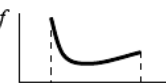
The mechanical component results from the resistance of the softer material to “ploughing” by asperities of the harder one. The adhesion component comes from adhesive bonds formed between the surfaces in the friction contact. It is believed that for polymers the adhesion (molecular) component exceeds much the mechanical one.¹⁵ This is explained by transfer films generated on the metal counterface. Special consideration is given to transfer films as the key factor which determines the tribological behavior of polymer materials.^{4,7} The following factors affect considerably the friction force: the contact load, sliding velocity, and temperature. The effects are not independent, for example, depending on the contact load and velocity the contact temperature may vary considerably changing the friction mode.

5.1. Effect of Load on Friction

It is a common knowledge that the friction force is proportional to the normal load and experiments have shown that this law is valid for some polymers (see Table 2). The friction coefficient remains practically constant under the load from 10 to 100 N when a steel ball of the radius 6.35 mm slides over polytetrafluoroethylene (PTFE), polymethyl methacrylate (PMMA), polyvinylchloride (PVC), polyethylene (PE), and Nylon.⁵⁵ Other authors^{56,57} have obtained similar results with the same materials as well as with some others, e.g. with PTFE, polytrifluorochloroethylene (PTFCE), PVC, polyvinyliden chloride (PVDC), and PE under the load from 2 to 15 N, with PTFE, PMMA, polystyrene (PS) and PE under the load from 10 to 40 N, and so on.

Outside this range, to the left and right, the proportionality between the friction force and applied load breaks down. Thus, it was shown that in the range of moderate loads 0.02 to 1 N the friction coefficient decreases with increasing the load.⁵⁸ Such a behavior may be explained by the elastic deformation of surface asperities. Of interest is the fact that similar behavior is characteristic of rubbers for which the elastic deformation is typical.^{59,60}

Table 2. Effect of load on friction coefficient.

Author(s)	Materials and load	Graphical representation
Bowers, Clinton, Zisman ⁵⁶	2–15 N Steel–polymer (PTFE, PFCE, PVC, PVDC, PE)	
Shooter, Thomas ⁵⁷	10–40 N Steel–polymer (PTFE, PE, PMMA, PC)	
Shooter, Tabor ⁵⁵	10–100 N Steel–polymer (PTFE, PE, PMMA, PVC, Nylon)	
Rees ⁵⁸	Steel–polymer (PTFE, PE, Nylon)	
Bartenev ⁵⁴ , Schallamach ⁶⁵	Theory Steel–rubber	
Kragelskii ⁴	Theory Steel–rubber	

On the other side of the proportionality range, the friction coefficient increases with increasing the load. This is often explained by the plastic deformation of asperities in the contact. Thus, the friction of polymers as a function of the load varies in the manner which was described by Kragelskii.⁴ That is, the friction coefficient passes the minimum which corresponds to transition from the elastic contact to plastic one.

We should bear in mind that the load can vary the temperature of visco-elastic transitions in polymers and thereby the mechanism of friction.

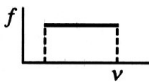
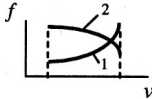

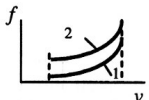

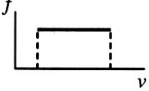
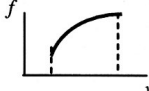
5.2. Effect of Sliding Velocity on Friction

Theoretically, the friction force should not depend on the sliding velocity. For polymers, however, this statement is only true if the

temperature within the contact area grows but negligibly. Usually there is a complex dependence of the friction coefficient on the velocity explained by variations in the relaxation properties and physicochemical activity of macromolecules. When the test temperature of the polymer sample approaches that of glass-transition a strong dependence of the friction coefficient on the velocity is observed. At lower temperatures f does not practically depend on the velocity.⁶¹

It is difficult to separate the effects of the velocity and temperature on friction. Examples of great diversity of the available results are shown in Table 3.

Table 3. Effect of sliding velocity on friction coefficient.

Author(s)	Materials and sliding velocity	Graphical representation
Shooter, Thomas ⁵⁷	0.01–1.0 cm/s Steel–polymer (PTFE, PE, PMMA, PC)	
Milz, Sargent ⁶⁶	4 – 183 cm/s Polymer–polymer 1 – Nylon, 2 – PC	
Fort ⁶⁸	10 ⁻⁵ –10 cm/s Steel–polymer (PTFE)	
White ⁶⁴	0.1 – 10 cm/s Steel–polymer (1 – PTFE, 2 – Nylon)	
Flom, Porile ^{62,63}	1.1– 180 cm/s Steel–polymer (PTFE)	
Oloffson, Gralben ⁶⁰	1.5 cm/s Polymer–polymer (fibers)	
Bartenev and Lavrentiev ⁵⁴ , Schallamach ⁵⁹	Theory Steel–rubber	

Velocity-independent friction occurs only within a limited range of velocities (0.01–1.0 cm/s) for PTFE, PE, PMMA, and PS⁵⁷ as well as for fiber-fiber contact.⁶⁰ But more complex relationships between the friction coefficient and sliding velocity are most often observed. Such relationships can be related to the visco-elastic behavior of polymers.

In the range of low velocities the viscous resistance in the contact zone increases with increasing the velocity. When the contact pressure is high, an abnormal viscous flow is observed which leads to a sharp rise in the viscosity due to an increase in the velocity.⁶²⁻⁶⁴ Molecular-kinetic considerations lead one to the same dependence.^{54,65}

In the range of high velocities, elastic behavior is prevalent in the contact zone and, as a result, the friction force depends only slightly on the velocity or it decreases with the velocity.^{66,67} In addition, it should be borne in mind that the duration of contact is short at high velocities leading to further decrease in the friction force.

In the intermediate range of velocities all the above factors are in competition and a maxima appears on the friction force–sliding velocity curve whose position depends on the relaxation properties of the polymer.⁸⁶

It should be recognized that the friction force–sliding velocity relationship depends essentially on the test temperature.⁶¹ When the tests are conducted near the glass-transition temperature the sliding velocity has a pronounced effect on friction whereas at lower temperatures friction hardly depends on the sliding velocity.

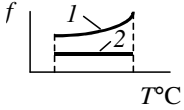
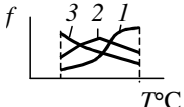
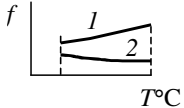
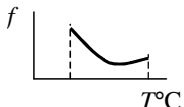
5.3. Effect of Temperature on Friction

Polymers as visco-elastic materials are very sensitive to frictional heating. It is commonly known that heat generation at friction results from the deformation of the material on real contact spots. Another source of heat can be attributed to the formation and rupture of adhesive bonds. These processes are most probably energetically non-equivalent and the energy difference may cause the generation or absorption of heat.

Often it is believed that the effect of temperature on friction can be taken into account using the mechanical characteristics of polymers measured at certain temperatures. In support of this assumption, a

correlation of the friction coefficient with the hardness and shear strength was found for some polymers.^{61,68,69} Such correlation is valid only when the temperature has no effect on adhesion.⁷⁰ Some friction patterns as functions of temperature are presented in Table 4.

Table 4. The effect of temperature on friction coefficient.

Author(s)	Material	Temperature, test conditions	Graphical representation
Shooter, Thomas ⁵⁷	1 – PS, 2 – PTFE	20–80°C Steel–polymer	
Ludema, Tabor ⁶⁹	1, 2 – PCTFE, 3 – PP	–50+150 °C Steel–polymer 1 – v = 3.5×10 ^{–5} cm/s, 2 – v = 3.5×10 ^{–2} cm/s	
King, Tabor ⁷⁰	1 – PE, 2 – PTFE	–40+20 °C Steel–polymer	
Schallamach ⁵⁹	Rubber	20–200 °C Steel–polymer	

6. Wear of Polymers

The main mechanisms of wear for polymers are adhesion, abrasion, and fatigue.^{4,7} Abrasive wear is caused by hard asperities on the counterface and/or hard particles that move over the polymer surface. This mode of wear occurs when the roughness is the determinative parameter in friction.

The adhesive mode of wear occurs in the sliding of a polymer over unlike surface, e.g. metal, when the strength of the adhesive bonds formed between the contacting materials can exceed the cohesive strength of the polymer. As a result, some part of the material is transferred onto the counterface and forms a transfer film; another part of the worn material is removed from the friction zone as the wear debris.

The fatigue wear of polymers is caused by the crack propagation at the repeated deformation of the material at friction. Fatigue results in the pitting, crack generation, and delamination. The wear debris are formed as a result of the growth and intersection of the small cracks on the polymer surface which are perpendicular to the sliding direction. The fatigue wear occurs after prolonged friction that may be important in the absence of adhesive wear when the counterface is smooth.

In general, three stages of wear can be distinguished:⁷¹ running-in, steady regime and catastrophic wear. As applied to a metal/polymer friction system, the first stage implies the generation of a transfer film on the metal counterface. For most metal/polymer systems the tribological characteristics much depend on the properties of the transfer film, i.e. its nature, strength of bonding to the metal surface, the part of the counterface area covered with the transfer film, the severity of adhesive interaction on the polymer/transfer film interface. This has been supported experimentally and reported by several authors.^{7,72,73}

As polymers adhere to hard surfaces through adsorption⁷⁴ it can be assumed that the adhesion component of the friction force depends on the adsorptivity of macromolecules. Immobilization of their functional groups and constraining the molecular mobility must affect strongly the tribological behavior of the polymer.

The friction of polymers over metals is greatly affected by tribochemical reactions occurring in the contact zone.⁷⁵ The tribochemical transformations in macromolecules follow the free-radical mechanism consisting of three main stages: initiation of macromolecules; growth of chains and their termination.

The direction and kinetics of chemical processes in polymers depend not only on the chemical structure of macromolecules but also on the arrangement of molecules, perfection and size of crystallites, the degree of molecular orientation, and molecular mobility. The structural heterogeneity in polymers leads to non-uniform distribution of additives and reagents in their bulk. In the partially crystalline polymers the low-molecular weight substances (oxygen, products of oxidation, inhibitors, plasticizers, dyes, fillers, etc.) tend to concentrate in the amorphous regions of the polymer; most reactive fragments of macromolecules are

also localized there. The local concentrations of reagents may differ much from the average concentrations; consequently, the local rates of tribochemical reactions must be different from the average rates. Thus, the introduction of additives into the polymer that alters its physical structure unavoidably affects its tribological properties. The tribochemical transformations in macromolecules and wear of polymer can be affected by the composition of the counterface metal. Effective catalysts of chemical processes in polymers that follow the radical mechanisms are Pt, Pd, Rh, Mo, Ta, Cr, and Ti. No effect is produced by Au and Ag. Quite typical tribochemical processes are hydrogenation (catalyzed by alloys containing Ni, Co, Fe, Cu, Pt, and Re), dehydrogenation (catalyzed by oxides of alkali-earth, transition metals and rare-earth elements; sulphides, tellurides, stibides, arsenides, selenides of Mg, Ca, Zn, Cd, Cr, Ni, Mo, etc; borides, nitrides, carbides, silicides, phosphides of V, Ti, Cr, Mo, W, etc); oxidation (partial oxidation is catalyzed by oxides of V–VIII groups of metals e.g. Mo, Bi, Co, Fe, etc). The compounds resulted from interaction of the macromolecules and the products of tribochemical reactions have various chemical structures. Often, especially at friction in air, these may be compounds of the coordination type. The coordination compounds generated on a surface seem typical enough for metal/polymer systems as this process is observed in the static contact between a polymer and metal.⁷⁵

6.1. Abrasive Wear

Abrasion displays scratches, gouges, and scoring marks on the worn surface; the debris produced by abrasion are frequently shaped as the fine cutting chips similar to those produced during machining, although at a much finer scale. Most of the models associated with abrasive wear incorporate geometric asperity descriptions, so that wear rates turn out to be quite dependent on the shape and apex angles of the abrasive points moving over the surface.

There are two distinct modes of deformation when an abrasive particle acts on the plastic material. The first mode is the plastic grooving

often referring to as ploughing. It occurs when a prow is pushed ahead of the particle and material is continually displaced sideways to form the ridges adjacent to the developing groove. No material is removed from the surface. The second mode is named the cutting because it is similar to micromachining and all the material displaced by the particle is removed as a chip.

There is another approach to description of abrasive wear. Experiments have shown that the abrasive wear rate is in proportion to $1/\sigma_u \epsilon_u$ where σ_u is the ultimate tensile stress and ϵ_u is the corresponding strain (see Fig. 7). The correlation was found by Lancaster and Ratner and is often referred to by their names.^{76,77}

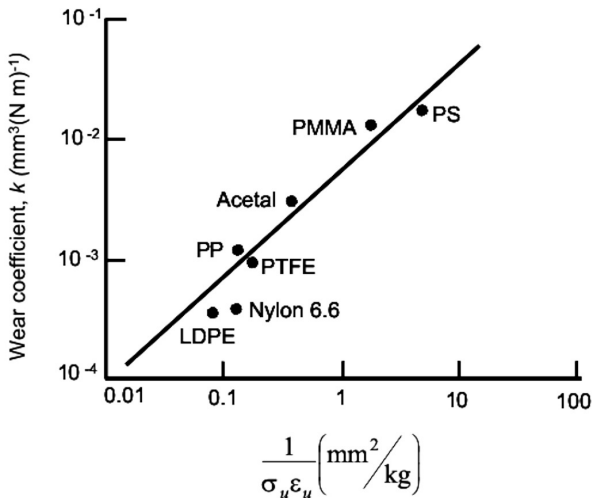


Fig. 7. Ratner-Lancaster correlation for abrasion: σ_u , ϵ_u are ultimate tensile stress and elongation (after Briscoe (1981)⁴³).

In two-body abrasion some asperities produce ploughing, the rest make cutting depending on two controlling factors: the attack angle of the particle and the interfacial shear strength expressed as the ratio between the shear stress at the interface and the shear yield stress of plastically deformed material. In the case of three-body abrasion the free abrasive particle readily penetrates the polymer surface which begins to operate as an emery cloth that increases the wear of the counterface.

6.2. Adhesive Wear and Friction Transfer

Adhesive wear results from the shear of friction junctions. This wear mode involves the formation of adhesive junctions, their growth and rupture. Belyi *et al.* noted that the transfer of a polymer is the most important characteristic of the adhesive wear of polymer-based materials¹⁵.

The phenomenon of friction transfer is observed for nearly all materials. The consequences of material transfer may be significantly distinct.⁷⁸⁻⁸⁰ If the small particles of micrometer size are transferred from one surface to the other the wear rate varies only slightly. Under certain conditions the situations take place such that a thin film of the soft material is transferred onto the hard mating surface, for example, polymer on metal. If the transferred polymer film is carried away from the steel surface and is continuously formed the wear rate increases. In the case when the film is held in place, the friction occurs between the similar materials which may eventually result in seizure. Spreading of the polymer on steel gives rise to an abrupt jump of the friction force but the wear changes insignificantly.

It has been known that under certain conditions the hard material is transferred on the soft surface. For example, bronze is transferred on polymer. The transferred hard particles are embedded in the soft material and act as the abrasive which scratches the parent material.

Friction transfer attracted a lot of attention in the tribological community generating many new concepts and hypotheses.⁸¹

Polymers are most susceptible to the friction transfer when rubbing both against metals and polymers. As an illustration let us consider friction between PTFE and PE.¹⁵ Experiments were carried on the wear tester with the block-on-ring geometry. It has been found that PTFE is transferred in the form of flakes of very small sizes during the initial period of friction. The thickness of the transferred film increases monotonically and then oscillates about a mean value; the magnitude and amplitude of the oscillations depend on the test conditions, especially on the load and sliding velocity (see Fig. 8).

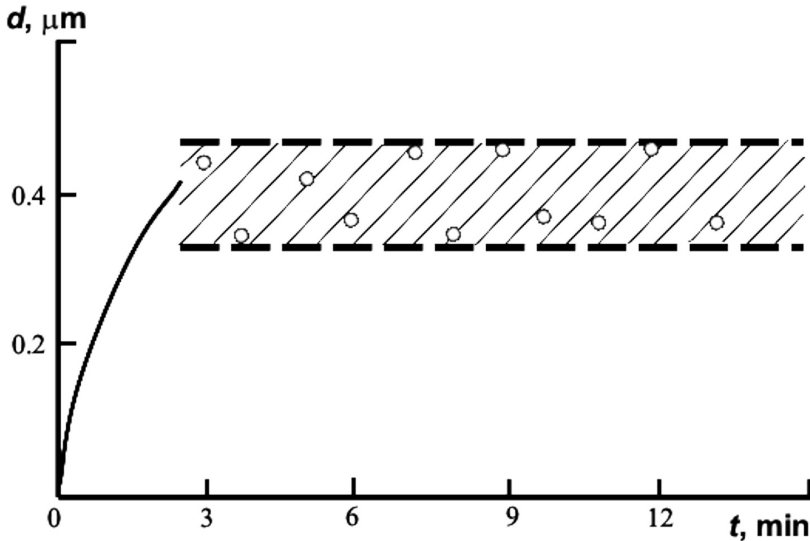


Fig. 8. Thickness of transferred film of PTFE as a function of friction duration (load = 0.05 MPa, sliding velocity = 0.35 m/s).

Self-lubricating additives such as PTFE are used to optimize the frictional properties of solids.⁸² It is important that the lubricant is transferred to the surface of the contact material during sliding reducing the interfacial shear stress and friction coefficient.

Figure 9a shows the well-known schematic representation of the semi-crystalline nature of PTFE.⁶ There are lamellae of crystalline layers with amorphous regions between them.

Figure 9b illustrates the AFM image of the PTFE surface after friction tests. Crystallites are clearly seen on the friction surface. They are disordered which proves their free motion occurred during friction. Therefore, the presence of free slices governs the reduction of the friction coefficient and frictional transfer for the materials filled with PTFE.

One more consequence of the polymer transfer is a change in the roughness of both surfaces in contact. The roughness of polymer surface undergo large variation during the unsteady wear until the steady wear is reached, while the roughness of the metal surface is modified due to the transfer of polymer.⁸³

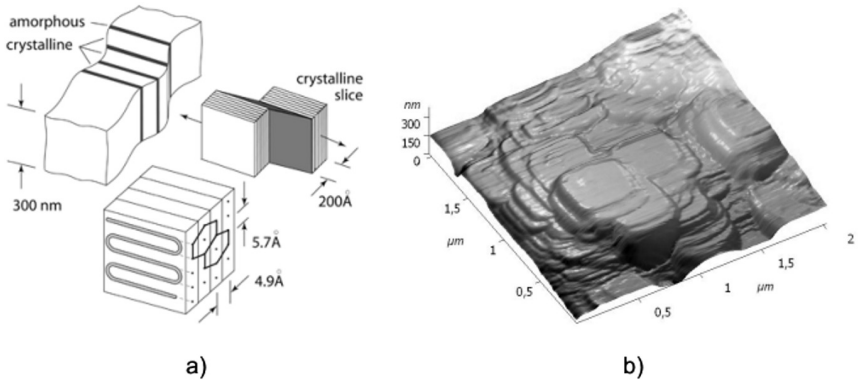


Fig. 9. a) Microstructure of PTFE; b) AFM-image of PTFE friction surface.

6.3. Fatigue Wear

The fatigue is known to be a change in the material state due to repeated stressing. Its characteristic feature is the accumulation of irreversible changes, which give rise to the generation, and the development of cracks. The similar process takes place during friction being named the friction fatigue. Unlike the bulk fatigue, it spans only the surface and sub-surface regions. It has been known that the fatigue cracks are initiated at the points where the maximum tangential stress or the tensile strain takes place. The theoretical and experimental studies show that under the contact loading the maximum tangential stress position is dependent on the friction coefficient.

With low friction coefficient, the point where the shear stress is maximal is located below the surface ($f < 0.3$). When the friction coefficient increases ($f > 0.3$), the point emerges on the surface. On the other hand, if a solid is subjected to a combination of the normal and tangential loading, the surface and sub-surface regions appear where the tensile strain and thereby the frictional heating occurs. Therefore, the cracks may be nucleated in surface and/or below it.^{26,27}

The initiation of the fatigue cracks is assisted by the defects, which are responsible for stress concentration. These are the scratches, dents,

marks and pits on the surface, and impurities, voids, cavities in sub-surface region. Both the surface and sub-surface cracks which open due to the repeated stressing will gradually grow, join, cross each other and meet the surface until the wear debris are detached after a certain number of the stressing cycles.

The fatigue wear rate is dependent on the numerous factors: physical, mechanical and chemical properties of solid surface, lubricant, environment, surface quality, temperature, etc. Although the friction force is decreased by lubrication and hence the tensile stress drops, the fatigue wear occurs and a number of cycles to the surface damage increases insignificantly.

6.4. Frictional Behaviour of Polymer Materials with Nanofillers

The reported data evidence a strong influence of nano-additives on the structure and properties of polymers. One of the most useful results achieved with the nano-dimensional fillers is increased mechanical properties (mechanical strength, modulus of elasticity) of polymer materials. This is especially pronounced with nanoclays and carbon nanomaterials.^{84,85} It is clearly proved at relatively low contents of the nanofiller. One of the main reasons for this is strong adsorptive interaction of macromolecules with rather developed filler surface, and also polymer transition to some particular conditions with constricted molecular mobility. The increased cohesive strength of the polymer binder can result in the improved tribological properties of the composites such as the abrasion resistance and resistance to fatigue wear.

The nano-particle fillers can markedly raise the heat distortion temperature (HDT) of polymer materials. For example, in the case of Nylon 6, HDT under loading increases from 65°C for the pure polymer up to 152°C for the nanocomposite containing montmorillonite (MMT) – 14.7 wt %.⁸⁶ An increase in heat resistance is also typical of non-polar polymers. For PP, for example, HDT rises from 109°C up to 152°C at a clay content of 6 wt %.⁸⁷ As the high temperature may develop in the friction contact zone, a rise in HDT must be favourable for tribological characteristics.

It was found that clay added to polymer materials enhances their heat resistance as well as the thermal resistance including the resistance to thermal-oxidative degradation.⁸⁴ The nanoparticles prevent oxygen from diffusion into the polymer and escape of the volatile products of thermolysis. It was also noticed that prolonged heating of a nanocomposite can strengthen the barrier quality owing to the backing of a silicate in the surface layer of the sample and result in a networked structure.⁸⁸

The inhibitive action of fullerenes and carbon nanomaterials with respect to thermal and thermal-oxidative degradation of polymer materials has been studied and is still under intensive study.^{89,90} Fullerenes are electrophilic being the active acceptors of electrons. They tend to accept nucleophilic reagents and also hydrogen, free-radical and carbenoidal particles. Therefore, fullerenes present in the surface layer of rubber must influence the course of the tribochemical transformations and consequently the friction parameters.

At strong adsorptive interaction of nanofillers and macromolecules the molecular mobility becomes abruptly frozen in the polymer amorphous phase. The functional groups in macromolecules become blocked by the interaction with the filler surface.⁸⁴ As a result, the obstacles are created that prevent from adhesive interaction with the counterface, and the adhesion component of friction force decreases.

The presence of nano-particles within a friction contact may influence the processes of the mass transfer, the accumulation of static electricity, the heat transfer on individual sites of contacting surfaces, the creation of real contact areas, *etc.*

Thus, effects of nano-fillers on the tribological properties of polymers can alter both bulk and surface properties of the materials.

7. Conclusions

A widespread interest in plastics has grown in the mid twentieth century due to the features of their structure, specific mechanical behavior, and considerable possibility to change the polymer properties. But, creep behavior of polymers (strong dependence of their properties on temperature), low heat conductivity, and sensitivity to the environment

often posed the numerous problems. The extensive studies over many years have developed the field of modern engineering in which the plastics can be applied as tribological materials, more commonly in the form of coatings and solid lubricants. The latter are used either in the pure form or as the composites or laminated structures.⁹¹ The thin polymer films, e.g. self-assembled monolayers formed by the chemisorption and physisorption of organic molecules (polymers) are prospective boundary lubricants in the fast-growing area of the memory storage devices, the microelectromechanical systems and other precision mechanisms.^{92,93}

Further progress in the field of friction and wear of polymers and their composites should be based on solving a number of the important problems which will allow us to establish more refined mechanisms which occur in the working surfaces of friction pairs. It appears important to study the structural changes at molecular level in the surface layers, and to investigate the tribo-chemical reactions. It is also important to find the methods of controlled regulation over the structure and frictional properties of polymers, based on the physical premises and concepts.

It is clear that the progress in engineering will provide many new opportunities in applications of plastics and therefore research in their mechanical and tribological behavior will be a challenging and fruitful field of science and technology.

Acknowledgments

Present work was partially funded under INTAS grant No 05-7940. This chapter was greatly inspired by the ideas of late Dr. M.I. Petrokovets (1937-2006).

References

1. B. J. Briscoe, in: *Friction and Wear of Polymer Composites*, Ed. F. Klaus (Elsevier, Amsterdam, 1986), p. 25.
2. B. J. Briscoe, in: *Fundamental of Friction: Macroscopic and Microscopic Processes*, Ed. I. L. Singer and H. M. Pollok (Kluwer Academic Publishers, Dordrecht, 1992), p. 167.

3. F. P. Bowden and D. Tabor, *Friction and Lubrication of Solids* (Clarendon Press, Oxford, 1964).
4. I. V. Kragelskii, *Friction and Wear* (Pergamon Press, Elmsford, 1982).
5. N. K. Myshkin, C. K. Kim and M. I. Petrokovets, *Introduction to Tribology* (CMG Publishers, Seoul, 1997).
6. L. S. Schadler, L. C. Brinson and W.G. Sawyer, *JOM*, **59**, 50 (2007).
7. S. Bahadur, *Wear*, **245**, 92 (2000).
8. S. Bahadur, and V. K. Polineni, *Wear*, **200**, 95, (1996).
9. A. A. Cenna, P. Dastoor, A. Beehag and N. V. Page, *J. Mater. Sci.*, **36**, 891 (2001).
10. H. S. Nalwa, *Encyclopedia of Nanoscience and Nanotechnology* (American Scientific Publishers, California, 2004).
11. Z. Zhang and K. Friedrich, in: *Polymer Composites – from Nano- to Macroscale* (Springer, Berlin 2005), p. 169.
12. K. W. Allen, *Phys. Technol.*, **19**, 234 (1988).
13. B. V. Deryagin, N. A. Krotova and V. P. Smilga, *Adhesion of Solids*, (Consultant Bureau, New York, 1978).
14. D. H. Buckley, *Surface Effects in Adhesion, Friction, Wear, and Lubrication*, (Elsevier, Amsterdam, 1981).
15. V. A. Bely, A. I. Sviridenok, M. I. Petrokovets and V. G. Savkin, *Friction and Wear in Polymer-Based Materials* (Pergamon Press, Oxford, 1982).
16. V. V. Tsukruk, H.-S. Ahn, D. Kim and A. Sidorenko, *Appl. Phys. Lett.*, **80**, 4825 (2002).
17. I. Luzinov, D. Julthongpiput, V. Gorbunov and V.V. Tsukruk, *Tribol. Int.*, **34**, 327 (2001).
18. M. Lemieux, S. Minko, D. Usov, M. Stamm, and V. V. Tsukruk, *Polymer Preprints*, **44**, 490 (2003).
19. Ya. E. Geguzin and N. N. Ovcharenko, *Sov. Phys. Usp.*, **5**, 129 (1962).
20. K. L. Johnson, K. Kendall and A. D. Roberts, *Proc. Roy. Soc.* **A324**, 301 (1971).
21. K. L. Johnson, *Contacts Mechanics*, (Cambridge University Press, Cambridge, 1987).
22. B. V. Deryagin, V. M. Muller and Yu. P. Toporov, *J. Colloid Interface Sci.*, **53**, 314 (1975).
23. K. L. Jonson and J. A. Greenwood, *J. Colloid Interf. Sci.*, **192**, 326 (1997).
24. D. Maugis, *J. Colloid Interf. Sci.*, **150**, 243 (1992).
25. I. M. Hutchings, *Tribology: Friction and Wear of Engineering Materials* (Edward Arnold, London, 1992).
26. Y. Yamaguchi, *Tribology of Plastic Materials* (Elsevier, Amsterdam, 1990).
27. N. K. Myshkin and M. I. Petrokovets, in *Mechanical Tribology. Materials, Characterization, and Applications*, Eds. G. E. Totten and H. Liang, (Marcel Dekker, New York and Basel, 2004).
28. M. I. Petrokovets, *Journal of Friction and Wear*, **20**, 1 (1999).
29. J. R. Barber, *Int. J. Mech. Sci.*, **15**, 813 (1973).

30. J. A. Greenwood and J. B. P. Williamson, *Proc. Roy. Soc.*, **A295**, 300 (1966).
31. J. A. Greenwood and J. H. Tripp, *ASME J. Appl. Mech.*, **34**, 153 (1967).
32. P. R. Nayak, *ASME J. of Lubrication Technology*, **93**, 398 (1971).
33. K. N. G. Fuller and D Tabor, *Proc. Roy. Soc.* **A345**, 327 (1975).
34. N. K. Myshkin, M. I. Petrokovets and S. A. Chizhik, *Tribol. Int.*, **31**, 79 (1998).
35. N. K. Myshkin, M. I. Petrokovets and SA Chizhik, *Tribol. Int.*, **32**, 379 (1999).
36. J. N. Israelachvili, *Intermolecular and Surface Forces* (Academic Press, London, 1991).
37. J. N. Israelachvili, *Surf. Sci. Rep.*, **14**, 109 (1992).
38. N. K. Myshkin, A. Ya. Grigoriev, A. M. Dubravin, O. Yu. Komkov, N. D. Spencer, and M. Tosatti, in *Proc. of 14th Int. Colloquium Tribology "Tribology and Lubrication Engineering"*, (Germany, Esslingen, 2004), p. 73.
39. N. K. Myshkin, A. V. Kovalev, I. N. Kovaleva and A. Ya. Grigoriev, in *Proc. of "Tribology of Surface Layers and Coatings"*, (Czech Republic, Prague, 2004), p. 3.
40. N. Myshkin, A. Kovalev, W. Scharff and M. Ignatiev, in *Proc. of 2nd Vienna International Conference "Micro- and Nano-Technology VIENNANO'07"*, (Austria, Vienna, 2007), p. 229.
41. N. K. Myshkin, A. V. Kovalev and W. Scharff, in *Proc. of 7th International Symposium INSYCONT'06*, (Poland, Krakow, 2006), p. 249.
42. V. E. Starzhynsky, A. M. Farberov, S. S. Pesetskii, S. A. Osipenko and V. A. Braginsky, *Precision Plastic Parts and Their Production Technology*, (Nauka i Tekhnika, Minsk, 1992) (in Russian).
43. B. J. Briscoe, *Tribology Int.*, **14**, 231, (1998).
44. G. Jintang, *Wear*, **245**, 100 (2000).
45. H. Unal, U. Sen and A. Mimaroglu, *Tribol. Int.*, **37**, 727 (2004).
46. H. Unal and A. Mimaroglu, *Mater. Des.*, **24**, 183 (2003).
47. Y. K. Chen, O. P. Modi, A. S. Mhay, A. Chrysanthou and J. M. O'Sullivan, *Wear*, **255**, 714 (2003).
48. C. J. Schwartz and S. Bahadur, *Wear*, **251**, 1532 (2001).
49. Y. M. Xu and B. G. Mellor, *Wear*, **251**, 1522 (2001).
50. B. J. Briscoe, L. Fiori, and E. Pelillo, *J. Phys. D: Appl. Phys.*, **31**, 2395 (1998).
51. H. Shulga, A. Kovalev, N. Myshkin, and V. V. Tsukruk, *European Polymer Journal*, **40**, 949 (2004).
52. A. Kovalev, H. Shulga, M. Lemieux, N. Myshkin, and V. V. Tsukruk, *J. Mater. Res.*, **19**, 716 (2004).
53. D. F. Moore, *The Friction and Lubrication of Elastomers*, (Pergamon Press, Oxford, 1972).
54. G. M. Bartenev and V. V. Lavrentev, *Friction and Wear of Polymers*, (Elsevier, Amsterdam, 1981).
55. K. Shooter and D. Tabor, *Proc. Roy. Soc.* **B65**, 661 (1952).
56. R. C. Bowers, W. C. Clinton, and W. A. Zisman, *Lubrication Eng.*, **5**, 204 (1953).
57. K. Shooter and R. H. Thomas, *Research*, **2**, 533 (1952).

58. B. L. Rees, *Research*, **10**, 331 (1957).
59. A. Schallamach, *Proc. Phys. Soc.* **B65**, 658 (1952).
60. B. Oloffson and N. Gralben, *Text. Res. J.*, **17**, 488 (1947).
61. G. V. Vinogradov, G. M. Bartenev, A. I. Elkin and V K Mikhaylov, *Wear*, **16**, 213 (1970).
62. D. G. Flom and N. T. Porile, *Nature*, **175**, 682 (1955).
63. D. G. Flom and N. T. Porile, *J. Appl. Phys.*, **26**, 1080 (1955).
64. N. S. White, *J. Res. Nat. Bur. Stand.*, **57**, 185 (1956).
65. A. Schallamach, *Proc. Phys. Soc.* **B66**, 1161 (1955).
66. W. C. Milz and L. E. Sargent, *Lubrication Eng.*, **11**, 313 (1955).
67. K Tanaka, *Wear*, **100**, 243 (1984).
68. T. Fort, *J. Phys. Chem.*, **66**, 1136 (1962).
69. K. C. Ludema and D. Tabor. *Wear*, **9**, 329 (1966).
70. R. T. King and D. Tabor. *Proc. Phys. Soc.* **B66**, 728 (1953).
71. I. V. Kragelskii, M. N. Dobychin and V. S. Kombalov, *Friction and Wear Calculation Methods*, (Pergamon Press, Oxford, 1982).
72. S. P. Gubin, Yu. A. Koksharov, G. B. Khomutov and G. Yu. Yurkov, *Russ. Chem. Rev.*, **74**, 489 (2005).
73. L. Yu and S. Bahadur, *Wear*, **214**, 245 (1998).
74. V. L. Vakula and L. M. Pritykin, *Physical Chemistry of Polymer Adhesion*, (Khimia, Moscow, 1984) (in Russian).
75. G. Heinicke, *Tribochemistry*, (Akademie-Verlag, Berlin, 1984).
76. J. K. Lancaster, *Proc. Instn. Mech. Engrs.*, **183**, 98 (1968).
77. S. B. Ratner, I. I. Farberova, O. V. Radyukevich and E. G. Lure, *Soviet Plastics*, vol. 7, 37 (1964) (in Russian).
78. K. R. Makinson and D. Tabor, *Proc. Roy. Soc.*, **A281**, 49 (1964).
79. A. I. Sviridenok, V. A. Bely, V. A. Smurugov, and V. G. Savkin, *Wear*, **25**, 301 (1973).
80. K. Tanaka, Y. Uchiyama and S. Toyooka, *Wear*, **23**, 153 (1973).
81. N. K. Myshkin, *Wear*, **245**, 116 (2000).
82. C. H. Surberg, E. Badisch and A. Pauschitz, in Proc. of 2nd Vienna International Conference "Micro- and Nano-Technology VIENNANO'07", (Vienna, Austria, 2007), p. 201.
83. V. K. Jain and S Bahadur, in *Proc. of International Conference on Wear of Materials*, (Dearborn, 1979), p. 581.
84. B. J. Briscoe and S. K. Sinha, in *Tribology of Polymeric Nanocomposites*, Ed. K. Friedrich and A. Schlarb (Elsevier, Amsterdam, 2008), p. 1.
85. B. Jurkowska, B. Jurkowski, P. Kamrowski, S. S. Pesetskii, V. N. Kowal, L. S. Pinchuk and Y. A. Olkhov, *J. Appl. Polym. Sci.*, **100**, 390 (2006).
86. Y. Kojima, A. Usuki, M. Kawasumi, A. Okada, T. Kuraucki and O. Kamigaito, *J. Polym. Sci. Part A. Polym. Chem.*, **31**, 983 (1993).

87. P. H. Nam, P. Maiti, M. Okamoto, T. Kotaka, M. Ohshima, A. Usuki, N. Hasegawa and H. Okamoto, *Polymer Engineering and Science*, **42**, 1907 (2002).
88. J. W. Gilman, T. Kashiwagi, E. P. Giannelis, E. Manias, S. Lomakin, J. D. Lichtenhan and P. Jones, in *Chemistry and Technology of Polymer Additives*, (Blackwell Science, Oxford, 1999), p. 249.
89. B. M. Ginzburg, L. A. Shibaev, O. F. Kireenko, A. A. Shepelevskii, E. Yu. Melenevskaya and V. L. Ugolkov, *Polym. Sci.* **A47**, 160 (2005).
90. B. Troitskii, A. Domrachev, L. V. Khokhlova and L. I. Anikina, *Polym. Sci.* **A43**, 964 (2001).
91. G. C. Pratt, in *Encyclopedia of Materials Science and Engineering*, Ed. M. B. Bever, (Pergamon Press, Oxford, 1986), p. 281.
92. V. V. Tsukruk, T. Nguen, M. Lemieux, J. Hazel, W. N. Weber, V. V. Shevchenko, N. Klimenko and E. Sheludko. in *Tribology Issues and Opportunities in MEMS*, Ed. B. Bhushan, (Kluwer Academic Publishers, Dodrecht, 1998), p. 607.
93. B. Bhushan. *Tribology and Mechanics of Magnetic Storage Devices*, (IEEE Press, Springer, New York, 1996).